Entanglement-Enhanced Phase Estimation without Prior Phase Information

G. Colangelo,[1] F. Martin Ciurana,[1] G. Puentes,[2] M. W. Mitchell,[1,3,*] and R. J. Sewell[1,†]

[1]ICFO-Institut de Ciencies Fotoniques, The Barcelona Institute of Science and Technology, 08860 Castelldefels (Barcelona), Spain
[2]Departamento de Física, Facultad de Ciencias Exactas y Naturales, Pabellón 1, Ciudad Universitaria, 1428 Buenos Aires, Argentina
[3]ICREA—Institució Catalana de Recerca i Estudis Avanćats, 08015 Barcelona, Spain

(Received 7 February 2017; published 9 June 2017)

We study the generation of planar quantum squeezed (PQS) states by quantum nondemolition (QND) measurement of an ensemble of ^{87}Rb atoms with a Poisson distributed atom number. Precise calibration of the QND measurement allows us to infer the conditional covariance matrix describing the F_y and F_z components of the PQS states, revealing the dual squeezing characteristic of PQS states. PQS states have been proposed for single-shot phase estimation without prior knowledge of the likely values of the phase. We show that for an *arbitrary* phase, the generated PQS states can give a metrological advantage of at least 3.1 dB relative to classical states. The PQS state also beats, for most phase angles, single-component-squeezed states generated by QND measurement with the same resources and atom number statistics. Using spin squeezing inequalities, we show that spin-spin entanglement is responsible for the metrological advantage.

DOI: 10.1103/PhysRevLett.118.233603

Estimation of interferometric phases is at the heart of precision sensing, and is ultimately limited by quantum statistical effects [1]. Entangled states can improve sensitivity beyond the "classical limits" that restrict sensing with independent particles, and a diversity of entangled states have been demonstrated for this task, including photonic squeezed states [2,3] and spin-squeezed states [4]. These give improved sensitivity for a narrow range of phases, but worsened sensitivity for most phases. Optical "NOON" states [5] give improved sensitivity over the whole phase range, but introduce additional phase ambiguity that increases with the size, and thus sensitivity advantage, of the NOON state. Recent proposals [6,7] suggest using *planar quantum squeezed* (PQS) states to obtain an entanglement-derived advantage for all phase angles, with no additional phase ambiguity. A natural application is in high-bandwidth atomic sensing [8,9], in which the precession angle may not be predictable in advance. PQS states may also be valuable for *ab initio* phase estimation using feedback [10–16].

Discussion of such states under the name "intelligent spin states" [17] predates modern squeezing terminology, and analogous states have been studied with optical polarization [18,19]. Generation of PQS states in material systems has been proposed using two-well Bose-Einstein condensates with tunable and attractive interactions [7], and using quantum nondemolition (QND) measurements [20]. The latter approach is a well-established technique for squeezing a single spin component [21–27]. Here we follow this strategy, using Faraday rotation QND measurements applied to an ensemble of cold atomic spins with $f = 1$ and subject to Poissonian number fluctuations. As the ensemble spin precesses about the x axis in an external magnetic field, we measure the y and z spin components to generate measurement-induced squeezing in these two components, creating a PQS state [28]. The resulting state has enhanced sensitivity to the precession angle, i.e., to a Zeeman-shift induced phase. The demonstrated PQS state beats the best possible classical state at any precession angle, and beats single-component spin-squeezed states when averaged over the possible angles. Spin-squeezing inequalities [7] detect spin entanglement in the PQS state, showing the sensing advantage requires spin entanglement.

A spin $\mathbf{F}$ obeys the Robertson uncertainty relation

$$\Delta F_y \Delta F_z \geq \frac{1}{2}|\langle[F_y, F_z]\rangle| = \frac{1}{2}|\langle F_x\rangle|. \tag{1}$$

Unlike the canonical Heisenberg uncertainly relation, the rhs of Eq. (1) may vanish, e.g., for $\langle F_x\rangle = 0$, with the consequence that two spin components, e.g., F_y and F_z, may be *simultaneously* squeezed, with the uncertainty absorbed by the third component, F_x, as illustrated in Fig. 1(b). We refer to a state fulfilling this condition as a PQS state. Following the approach of He *et al.* [7,29], we adopt an operational definition planar squeezing. We take $\Delta^2 F_y = \Delta^2 F_z = F_{||}/2$ as the standard quantum limit, where $F_{||} \equiv \sqrt{\langle F_y\rangle^2 + \langle F_z\rangle^2}$, so that $F_{||}$ is the magnitude of the in-plane spin components. We define the planar variance $\Delta^2 F_{||} \equiv \Delta^2 F_y + \Delta^2 F_z$, with standard quantum limit $\Delta^2 F_{||} = F_{||}$, and the planar squeezing parameter $\xi_{||}^2 \equiv \Delta^2 F_{||}/F_{||}$. A PQS state has $\xi_{||}^2 < 1$, and has individual component variances below the standard quantum limit, i.e., $\xi_y^2 < 1$, and $\xi_z^2 < 1$, where $\xi_i^2 \equiv 2\Delta^2 F_i/F_{||}$, so that $\xi_{||}^2 = (\xi_y^2 + \xi_z^2)/2$.

A PQS state may be used to measure arbitrary phase angles with quantum-enhanced precision. Here we consider an ensemble of atomic spins precessing in the y-z plane in an external magnetic field B_x. The spin projection onto the

z axis is given by $F_z(t) = F_z \cos\phi - F_y \sin\phi$, where F_y and F_z are evaluated at $t = 0$ and the phase $\phi = \omega_L t$ is proportional to the magnetic field. The uncertainty in estimating ϕ of the atomic precession is

$$\Delta^2\phi = \frac{\Delta^2 F_z(\phi)}{|d\langle F_z(\phi)\rangle/d\phi|^2} = \frac{\Delta^2 F_z(\phi)}{(\langle F_y\rangle \cos\phi + \langle F_z\rangle \sin\phi)^2}, \tag{2}$$

where $\Delta^2 F_z(\phi) \equiv \Delta^2 F_y \sin^2\phi + \Delta^2 F_z \cos^2\phi + \mathrm{cov}(F_y, F_z) \sin 2\phi$, and $\mathrm{cov}(A,B) \equiv \frac{1}{2}\langle AB + BA\rangle - \langle A\rangle\langle B\rangle$ is the covariance. The standard quantum limit is $\Delta^2\phi_{\mathrm{SQL}} = 1/2F_{||}$. We note that PQS states reduce the planar variance for arbitrary angles on a finite interval, except where the denominator in Eq. (2) is equal to zero. In contrast, squeezing a single spin component is only beneficial to refine the estimate of a phase over a limited range of angles, and requires prior knowledge of the phase, or adaptive procedures to determine the phase during the measurement [29,30].

In our experiment, we measure the $F_z(t)$ spin projection of the precessing atomic spins via off-resonant paramagnetic Faraday rotation using a train of μs-duration optical probe pulses. We assume the probe duration is short compared to the Larmor precession period. The effective atom-light interaction is given by the Hamiltonian

$$H_{\mathrm{eff}} = g S_z F_z(t). \tag{3}$$

Here, the atoms are described by the collective spin operators $\mathbf{F} \equiv \sum_i \mathbf{f}^{(i)}$, with $\mathbf{f}^{(i)}$ the spin orientation of individual atoms. The optical polarization of the probe pulses is described by the Stokes operators $S_k = \frac{1}{2}(a_L^\dagger, a_R^\dagger)\sigma_k(a_L, a_R)^T$, with Pauli matrices σ_k. The coupling constant g depends on the detuning from the resonance of the probe beam, the atomic structure, and the geometry of the atomic ensemble and probe beam [31–33].

Equation (3) describes a QND measurement of $F_z(t)$ [34]: an input S_x-polarized optical pulse interacting with the atoms experiences a rotation by an angle $\theta = gF_z(t)$; measurement of θ projects the atoms onto a state with $\Delta^2 F_z(t)$ reduced by a factor $1/(1 + g^2 N_A n_l)$, where n_l is the number of photons in a single probe pulse, $\Delta^2 F_x(t)$ increased by a factor $1 + g^2 n_l$, and $\Delta^2 F_y(t)$ increased by a negligible factor of order 1. Repeated QND measurements of $F_z(t)$ during multiple Larmor precession cycles are used to produce a PQS state.

We work with up to 1.75×10^6 laser-cooled ^{87}Rb atoms held in a single beam optical dipole trap [31], as illustrated in Fig. 1(a). The atoms are initially polarized via high efficiency (~98%) stroboscopic optical pumping, in the presence of a small magnetic field applied along the x axis, such that $\langle F_y\rangle \simeq \langle N_A\rangle$. N_A is subject to Poissonian fluctuations because accumulation of independent atoms into the ensemble is a stochastic process limited by Poisson statistics $\Delta^2 N_A = \langle N_A\rangle$. We refer to this kind of state as a

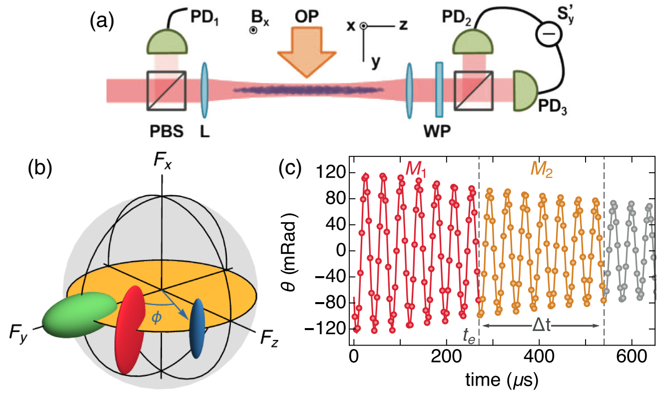

FIG. 1. (a) Experimental setup. A cloud of laser-cooled ^{87}Rb atoms is held in a singe-beam optical dipole trap. The atoms precess in the y-z plane due to an external magnetic field B_x. Optical probe pulses experience Faraday rotation by an angle $\theta \propto F_z(t)$, detected via measurement of the output Stokes parameter S_y' using a balanced polarimeter that consists in a wave plate (WP), a polarizing beam splitter (PBS), and photodiodes PD$_2$ and PD$_3$. The input S_x polarization is recorded with a reference photodetector (PD$_1$). (b) Illustration of a PCS state (green) with $\Delta^2 F_z = \langle N_A\rangle/2$ and $\Delta^2 F_y = \langle N_A\rangle$; a PSS state (red) with reduced $\Delta^2 F_z$ and increased $\Delta^2 F_y$; and a PQS state (blue) with both $\Delta^2 F_y$ and $\Delta^2 F_z$ reduced. Additional spin noise due to measurement back-action is directed into the F_x spin component, i.e., out of the plane, and does not enter into the measurement record. (c) Recorded measurements of the Faraday rotation angle from a precessing PCS state. We use the measurement record to predict the F_z and F_y components at a time $t = t_e$ using two sequential measurements M_1 and M_2 of duration Δt.

Poissonian coherent spin (PCS) state, with variances $\Delta^2 F_x = \Delta^2 F_z = \langle N_A\rangle/2$ and $\Delta^2 F_y = \langle N_A\rangle$. Generating sub-Poissonian atom number statistics, either via strong interaction among the atoms during accumulation [35–38], or as here, via precise nondestructive measurement [39,40], remains a significant experimental challenge.

We probe the atoms using a train of $\tau = 0.6$ μs duration pulses of linearly polarized light, with a detuning of 700 MHz to the red of the ^{87}Rb D_2 line, sent through the atomic cloud at 3 μs intervals. The probe pulses are V polarized, with on average $n_l = 2.74 \times 10^6$ photons. Between the probe pulses, we send H-polarized compensation pulses with on average $n_l^{(H)} = 1.49 \times 10^6$ photons through the atomic cloud to compensate for tensor light shifts [41]. During the measurement, an external magnetic field B_x coherently rotates the atoms in the y-z plane at the Larmor frequency ω_L. The time taken to complete a single-pulse measurement is small compared to the Larmor precession period, i.e., $\tau \ll T_L$. Off-resonant scattering of probe photons during the measurement leads to decay of the atomic coherence at a rate $\eta = 3 \times 10^{-10}$ per photon. The transformation produced by Eq. (3) is $S_y' = S_y \cos\theta + S_x \sin\theta$. In our experiment, we measure S_x at the input by picking off a fraction of the optical

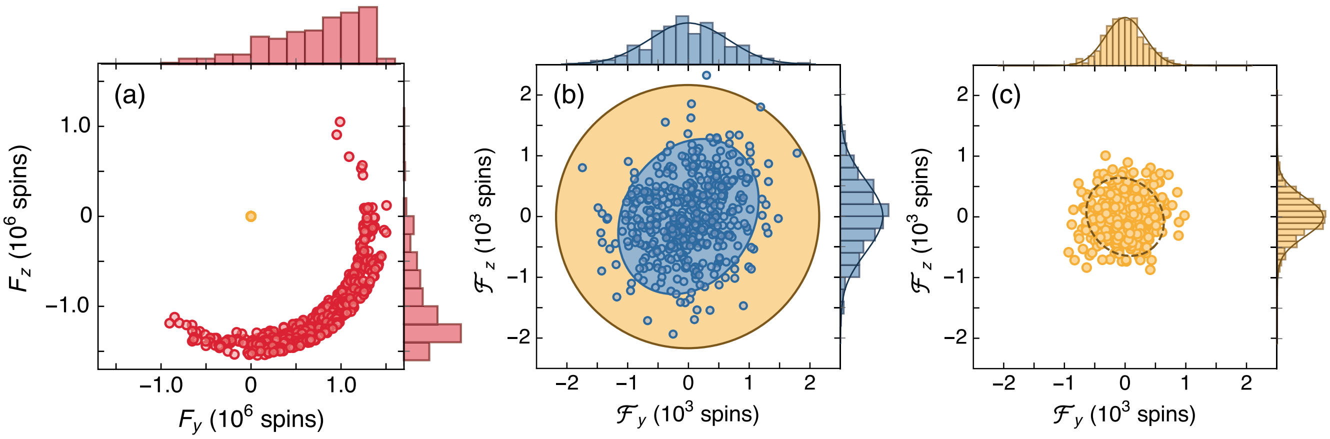

FIG. 2. (a) Spin state $\mathbf{F}_1$ (red dots) estimated at time t_e for an input state with $\langle N_A \rangle = 1.75 \times 10^6$ atoms from the 453 repetitions of the experiment. For comparison, we illustrate the corresponding measurement made without atoms in the trap, used to quantify the read-out noise (yellow dot). (b) Error in the best linear predictor, $\boldsymbol{F}$, of $\mathbf{F}_2$ given $\mathbf{F}_1$ (blue dots). The blue ellipse shows the measured 2σ radii of the distribution. The yellow ellipse shows the standard quantum limit $\Delta^2 F_y = \Delta^2 F_z = F_{||}/2$ with 2σ radii, where $\sigma^2 = (F_{||}/2)^2 + \Delta^2\theta_0$ and $\Delta^2\theta_0$ is the measured read-out noise. (c) Linear predictor $\boldsymbol{F}$ estimated from repeating the experiment without atoms in the trap, allowing quantification of the measurement read-out noise. The dashed ellipse shows the measured 2σ radii of the distribution.

pulse and sending it to a reference detector, and S_y' using a fast home-built balanced polarimeter [42]. Both signals are recorded on a digital oscilloscope, from which we calculate $\hat{\theta} = \arcsin(S_y'/S_x)$, the estimator for θ. We correct for slow drifts in the polarimeter signal by subtracting a baseline from each pulse, estimated by repeating the measurement without atoms in the trap.

The measurable signal is described by the free induction decay model [43]

$$\theta(t) = g(F_z(t_e)\cos\phi - F_y(t_e)\sin\phi)e^{-t_r/T_2} + \theta_0, \quad (4)$$

where $t_r \equiv t - t_e$ and the phase $\phi = \omega_L t_r$ is proportional to the magnetic field. We record a set of measurements $\theta(t_k)$, and detect the PQS state at time t_e. A typical free induction decay signal is illustrated in Fig. 1(c). An independent measurement is used to calibrate g, while ω_L, T_2, and θ_0 are found by fitting the measured $\theta(t_k)$ over all the data points.

The model described in Eq. (4) allows a simultaneous estimation of $\mathbf{F}_1 = (F_y^{(1)}, F_z^{(1)})$ at a time $t = t_e$ by fitting the data using the measurements from an interval Δt *prior* to t_e (labeled M_1 in Fig. 1), producing a conditional PQS state at time t_e. We detect the PQS state by comparing the first measurement outcome to a second estimate $\mathbf{F}_2 = (F_y^{(2)}, F_z^{(2)})$ using the measurements from an interval Δt *after* to t_e (labeled M_2 in Fig. 1). The classical parameters g, ω_L, T_2, and θ_0 are fixed beforehand. As a result, these are two linear, least-squares estimates of the vector $\mathbf{F}$ obtained from disjoint data sets [28].

From the measurement record, we compute the conditional covariance matrix $\Gamma_{\mathbf{F}_2|\mathbf{F}_1} = \Gamma_{\mathbf{F}_2} - \Gamma_{\mathbf{F}_2\mathbf{F}_1}\Gamma_{\mathbf{F}_1}^{-1}\Gamma_{\mathbf{F}_1\mathbf{F}_2}$ which quantifies the error in the best linear prediction of $\mathbf{F}_2$ based on $\mathbf{F}_1$ [44]. $\Gamma_{\mathbf{v}}$ indicates the covariance matrix for vector $\mathbf{v}$, and Γ_{uv} indicates the cross-covariance matrix for vectors $\mathbf{u}$ and $\mathbf{v}$. The difference between the best linear prediction of $\mathbf{F}$ using $\mathbf{F}_1$ and the confirming estimate $\mathbf{F}_2$ is visualized using the vector $\boldsymbol{F} = \{\mathcal{F}_y, \mathcal{F}_z\} = \tilde{\mathbf{F}}_2 - \Gamma_{\mathbf{F}_2\mathbf{F}_1}\Gamma_{\mathbf{F}_1}^{-1}\tilde{\mathbf{F}}_1$, where $\tilde{\mathbf{F}}_i = \mathbf{F}_i - \langle \mathbf{F}_i \rangle$. Statistics are gathered over 453 repetitions of the experiment. The atomic quantum noise contribution is calibrated via independent measurements, taking into account the inhomogeneous atom-light coupling [28]. Standard errors in the estimated conditional covariance matrix are calculated from the statistics of $\{\boldsymbol{F}\}$.

The estimate of the state from the two independent measurements is subject to technical noise due to amplitude and phase fluctuations of the input state, and shot-to-shot variations of the magnetic field. In Fig. 2(a), we plot the estimate of $\mathbf{F}_1$ at time t_e for an input state with $\langle N_A \rangle = 1.75 \times 10^6$ atoms. In contrast, the conditional uncertainty of $\mathbf{F}_2$ given $\mathbf{F}_1$ is limited mainly by the measurement read-out noise, as shown in Figs. 2(b) and 2(c). Empirically, we find $\Delta t = 270$ μs minimizes the total variance $\mathrm{Tr}(\Gamma_{\mathbf{F}_2|\mathbf{F}_1})$. This reflects a trade-off of photon shot noise versus scattering-induced decoherence and magnetic-field technical noise. At this point, $N_L = 2.47 \times 10^8$ photons have been used in the measurement and the atomic state coherence has decayed by a factor $\chi_{\mathrm{sc}} = 0.89$ due to off-resonant scattering, and a factor $\chi_{\mathrm{dec}} = 0.93$ due to dephasing induced by magnetic field gradients [45]. The resulting spin coherence of the PQS state is $F_{||} = \chi_{\mathrm{dec}}\chi_{\mathrm{sc}} N_A = 1.45 \times 10^6$ spins. The conditional covariance (in units of spins^2) is

$$\Gamma_{\mathbf{F}_2|\mathbf{F}_1} = \left[\begin{pmatrix} 2.32 & 0.64 \\ 0.64 & 3.00 \end{pmatrix} \pm \begin{pmatrix} 0.21 & 0.16 \\ 0.16 & 0.28 \end{pmatrix}\right] \times 10^5. \quad (5)$$

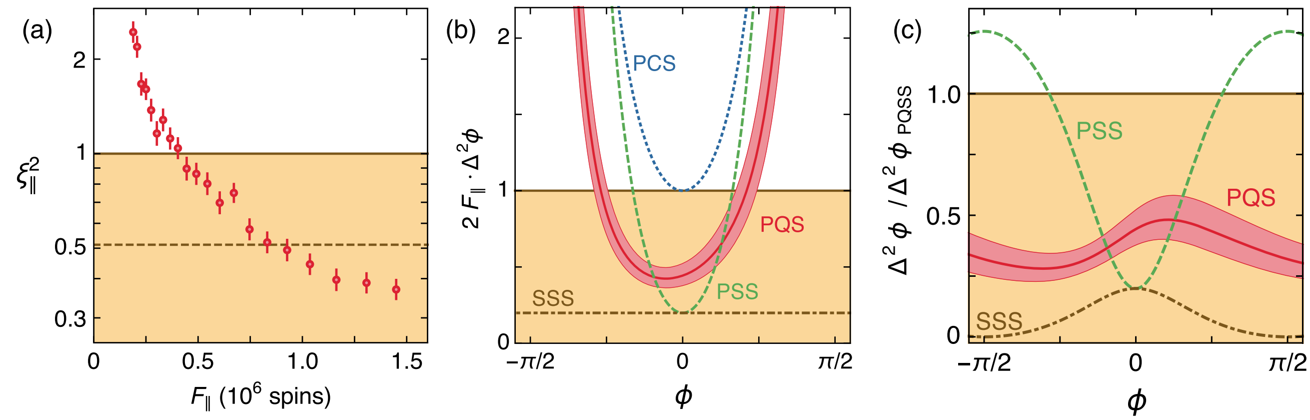

FIG. 3. (a) Semi-log plot of the planar squeezing parameter, $\xi_{||}^2$, as a function of the in-plane coherence $F_{||}$ of the atomic ensemble. We vary $F_{||}$ by changing the number of atoms loaded in the optical dipole trap. A PQS state is detected for $\xi_{||}^2 < 1$ (shaded region). Entanglement is detected for $\xi_e^2 = (F_{||}/\langle\tilde{N}_A\rangle)\xi_{||}^2 < 7/16$ (dashed line). Error bars represent $\pm 1\sigma$ statistical errors. (b) Calculated phase sensitivity of the PQS state as a function of the measurement phase ϕ (red solid line). The standard quantum limit $2F_{||}\Delta^2\phi = 1$ is indicated by the solid yellow line. We also show the phase sensitivity of the input PCS (blue dotted line), a PSS state produced with the same resources (green dashed line), and an ideal spin-squeezed state (SSS) not subject to number fluctuations (dark yellow dot-dashed line). (c) Metrologically significant *enhancement* in phase sensitivity relative to that of the PCS, $\Delta^2\phi/\Delta^2\phi_{\mathrm{PCS}}$, for the PQS (red solid line), PSS (green dashed line) and SSS (dark yellow dot-dashed line) states. Shaded bands indicate $\pm 1\sigma$ confidence intervals.

For comparison, the estimated read-out noise is

$$\Gamma_0 = \left[\begin{pmatrix} 1.02 & 0.14 \\ 0.14 & 1.03 \end{pmatrix} \pm \begin{pmatrix} 0.07 & 0.05 \\ 0.05 & 0.07 \end{pmatrix}\right] \times 10^5. \quad (6)$$

We note that $\Gamma_{\mathbf{F}_2|\mathbf{F}_1}$ allows for accurate characterization of the atomic state *given* accurate knowledge of the classical parameters g, ω_L, T_2, and θ_0. With better control of the magnetic field environment [46,47], these parameters could also be calibrated via independent measurements.

From $\Gamma_{\mathbf{F}_2|\mathbf{F}_1}$ we estimate the planar squeezing parameter $\xi_{||}^2 = \mathrm{Tr}(\tilde{\Gamma}_{\mathbf{F}_2|\mathbf{F}_1})/F_{||}$, where $\tilde{\Gamma}_{\mathbf{F}_2|\mathbf{F}_1} = \Gamma_{\mathbf{F}_2|\mathbf{F}_1} - \Gamma_0$ and $F_{||}$ is estimated at t_e. Γ_0 is the read-out noise, quantified by repeating the measurement without atoms in the trap. In Fig. 3(a) we show $\xi_{||}^2$ as a function of the in-plane coherence $F_{||}$ of the atomic ensemble, which we vary by changing the number of atoms in the optical dipole trap. We detect a PQS state for $F_{||} \geq 4 \times 10^5$ spins. With the maximum coherence $F_{||} = 1.45 \times 10^6$ spins, we observe $\xi_{||}^2 = 0.37 \pm 0.03 < 1$, detecting a PQS state with $> 20\sigma$ significance, with $\xi_y^2 = 0.32 \pm 0.03$ and $\xi_z^2 = 0.42 \pm 0.04$.

Entanglement is detected using the witness $\xi_e^2 \equiv \Delta^2 F_{||}/\langle\tilde{N}_A\rangle$, derived in Ref. [7]; for an ensemble of atoms with individual spin $f = 1$, entanglement is detected if $\xi_e^2 < 7/16$. Here $\tilde{N}_A \equiv [\chi_{\mathrm{sc}} + p(1-\chi_{\mathrm{sc}})]N_A$ is the number of atoms remaining in the $f = 1$ state after probing, $\chi_{\mathrm{sc}} \equiv 1 - \exp(\eta N_L)$ accounts for off-resonant scattering of atoms at a rate η, and p is the fraction of scattered atoms that return to $f = 1$ [45]. We measure $\xi_e^2 = 0.32 \pm 0.02 < 7/16$, detecting entanglement among the atomic spins with $> 5\sigma$ significance [7].

We also define a metrological squeezing parameter $\xi_m^2 \equiv F\Delta^2 F_{||}/F_{||}^2$, where $F \equiv \langle N_A\rangle$ is the input spin coherence, similar to the Wineland criterion [48,49], in that it compares noise to the magnitude of the coherence $F_{||}$. A PQS state with $\xi_m^2 < 1$ gives enhanced metrological sensitivity to arbitrary phase shifts. We observe $\xi_m^2 = 0.45 \pm 0.03$, indicating that entanglement-enhanced phase sensitivity is achievable.

To estimate the enhancement in phase sensitivity achievable using the observed PQS state, we evaluate Eq. (2) using the conditional covariance $\tilde{\Gamma}_{\mathbf{F}_2|\mathbf{F}_1}$ and the measured coherences. The PQS state achieves a maximum achievable sensitivity $\Delta^2\phi = (0.38 \pm 0.02)\Delta^2\phi_{\mathrm{SQL}}$, or $\Delta\phi = (3.6 \pm 0.1) \times 10^{-4}$ radians, at a phase $\phi = 0.68\pi$ radians. Note that this phase is determined by the choice of measurement time t_e. In Fig. 3(b) we plot the calculated phase sensitivity $\Delta^2\phi$ of the observed PQS state (red solid line). For comparison purposes, we rotate the PQS state so that the spin coherence is aligned along the y axis, i.e., $\mathbf{F} \to R(\theta) \cdot \mathbf{F}$ and $\Gamma_{\mathbf{F}_2|\mathbf{F}_1} \to R(\theta) \cdot \Gamma_{\mathbf{F}_2|\mathbf{F}_1} \cdot R(\theta)^T$, where $\arctan\theta \equiv F_y/F_z$. We compare this with the sensitivity of a PCS state with input spin coherence $\langle F_y\rangle = N_A$ (blue dashed line), and a Poissonian spin-squeezed (PSS) state, i.e., a state produced by squeezing the F_z component of the PCS state via an ideal QND measurement with the same measurement resources, with $\Delta^2 F_y = \langle N_A\rangle$, $\Delta^2 F_z$ reduced by a factor $1/(1 + g^2 N_L N_A/2)$, and input coherence $\langle F_y\rangle = \chi_{\mathrm{sc}} N_A$ (green dot-dashed line).

In Fig. 3(c) we plot the calculated *enhancement* in phase sensitivity $\Delta^2\phi$ of both the PQS and PSS states relative to the classical input PCS. The observed PQS state can provide ≥ 3.1 dB quantum-enhanced, metrologically significant phase sensitivity with respect to the PCS for all phases, with a maximum of 4.1 dB, enabling quantum-enhanced measurement of an *arbitrary* phase shift. In contract, the PSS state gives 6.6 dB enhancement relative to the PCS at $\phi = 0$, but performs worse than the PQS state outside the range $-0.09\pi < \phi < 0.12\pi$ radians.

In contrast to the well-known spin-squeezed states, planar quantum squeezed states enhance the precision of phase estimation without requiring *a priori* information about the phase. Here we have shown that QND measurement can efficiently produce such states, demonstrating that more than 3 dB of advantage relative to classical states is possible over the full range of phase angles. We also detect spin-spin entanglement, required for the metrological advantage. Such states are attractive for high-bandwidth and high-sensitivity optical magnetometers [8,50] and other atomic sensing applications employing nondestructive spin detection [16,26,51]. In our experiment, uncertainty in the spin coherence is dominated by Poissonian number fluctuations. In scenarios where uncertainty from measurement induced back-action due to curvature of the Bloch sphere is dominant [27], allocating measurement resources to squeezing the spin coherence, as in our strategy, may help to improve phase precision even for small angles, and to implement adaptive measurement strategies [13].

We thank Q. Y. He, M. Reid, P. Drummond, G. Vitagliano, G. Tóth, E. Distante, V. G. Lucivero, L. Bianchet, N. Behbood, and M. Napolitano for helpful discussions. The authors acknowledge financial support from the Spanish Ministry of Economy and Competitiveness, through the "Severo Ochoa" Programme for Centres of Excellence in R&D (SEV-2015-0522). This work was supported by MINECO/FEDER, MINECO projects MAQRO (Ref. FIS2015-68039-P), XPLICA (FIS2014-62181-EXP), the CERCA Programme/Generalitat de Catalunya, Catalan 2014-SGR-1295, by the European Union Project QUIC (Grant Agreement No. 641122), European Research Council project AQUMET (Grant Agreement No. 280169) and ERIDIAN (Grant Agreement No. 713682), and by Fundació Privada CELLEX. G. P. gratefully acknowledges funding from the Agencia Nacional de Promoción Científica y Tecnológica (ANPCyT), PICT2014-1543, PICT2015-0710, and UBACYT PDE 2017.

*morgan.mitchell@icfo.es
†robert.sewell@icfo.eu

[1] H. M. Wiseman and G. J. Milburn, *Quantum Measurement and Control* (Cambridge University Press, Cambridge, England, 2010).
[2] R. E. Slusher, L. W. Hollberg, B. Yurke, J. C. Mertz, and J. F. Valley, Observation of Squeezed States Generated by Four-Wave Mixing in an Optical Cavity, Phys. Rev. Lett. **55**, 2409 (1985).
[3] L.-A. Wu, H. J. Kimble, J. L. Hall, and H. Wu, Generation of Squeezed States by Parametric Down Conversion, Phys. Rev. Lett. **57**, 2520 (1986).
[4] V. Meyer, M. A. Rowe, D. Kielpinski, C. A. Sackett, W. M. Itano, C. Monroe, and D. J. Wineland, Experimental Demonstration of Entanglement-Enhanced Rotation Angle Estimation Using Trapped Ions, Phys. Rev. Lett. **86**, 5870 (2001).
[5] M. W. Mitchell, J. S. Lundeen, and A. M. Steinberg, Super-resolving phase measurements with a multiphoton entangled state, Nature (London) **429**, 161 (2004).
[6] G. Tóth, C. Knapp, O. Gühne, and H. J. Briegel, Spin squeezing and entanglement, Phys. Rev. A **79**, 042334 (2009).
[7] Q. Y. He, S.-G. Peng, P. D. Drummond, and M. D. Reid, Planar quantum squeezing and atom interferometry, Phys. Rev. A **84**, 022107 (2011).
[8] V. Shah, G. Vasilakis, and M. V. Romalis, High Bandwidth Atomic Magnetometery with Continuous Quantum Nondemolition Measurements, Phys. Rev. Lett. **104**, 013601 (2010).
[9] R. J. Sewell, M. Koschorreck, M. Napolitano, B. Dubost, N. Behbood, and M. W. Mitchell, Magnetic Sensitivity beyond the Projection Noise Limit by Spin Squeezing, Phys. Rev. Lett. **109**, 253605 (2012).
[10] J. K. Stockton, J. M. Geremia, A. C. Doherty, and H. Mabuchi, Robust quantum parameter estimation: Coherent magnetometry with feedback, Phys. Rev. A **69**, 032109 (2004).
[11] T. Takano, S.-I.-R. Tanaka, R. Namiki, and Y. Takahashi, Manipulation of Nonclassical Atomic Spin States, Phys. Rev. Lett. **104**, 013602 (2010).
[12] G. Y. Xiang, B. L. Higgins, D. W. Berry, H. M. Wiseman, and G. J. Pryde, Entanglement-enhanced measurement of a completely unknown optical phase, Nat. Photonics **5**, 43 (2011).
[13] J. Borregaard and A. S. Sørensen, Near-Heisenberg-Limited Atomic Clocks in the Presence of Decoherence, Phys. Rev. Lett. **111**, 090801 (2013).
[14] A. A. Berni, T. Gehring, B. M. Nielsen, V. Händchen, M. G. A. Paris, and U. L. Andersen, *Ab initio* quantum-enhanced optical phase estimation using real-time feedback control, Nat. Photonics **9**, 577 (2015).
[15] K. C. Cox, G. P. Greve, J. M. Weiner, and J. K. Thompson, Deterministic Squeezed States with Collective Measurements and Feedback, Phys. Rev. Lett. **116**, 093602 (2016).
[16] J. Kohler, N. Spethmann, S. Schreppler, and D. M. Stamper-Kurn, Cavity-Assisted Measurement and Coherent Control of Collective Atomic Spin Oscillators, Phys. Rev. Lett. **118**, 063604 (2017).
[17] C Aragone, G Guerri, S Salamo, and J. L. Tani, Intelligent spin states, J. Phys. A **7**, L149 (1974).
[18] N. Korolkova, G. Leuchs, R. Loudon, T. C. Ralph, and C. Silberhorn, Polarization squeezing and continuous-variable polarization entanglement, Phys. Rev. A **65**, 052306 (2002).
[19] R. Schnabel, W. P. Bowen, N. Treps, T. C. Ralph, H.-A. Bachor, and P. K. Lam, Stokes-operator-squeezed continu-

ous-variable polarization states, Phys. Rev. A **67**, 012316 (2003).

[20] G. Puentes, G. Colangelo, R. J Sewell, and M. W Mitchell, Planar squeezing by quantum non-demolition measurement in cold atomic ensembles, New J. Phys. **15**, 103031 (2013).

[21] A. Kuzmich, L. Mandel, and N. P. Bigelow, Generation of Spin Squeezing via Continuous Quantum Nondemolition Measurement, Phys. Rev. Lett. **85**, 1594 (2000).

[22] S. Chaudhury, G. A. Smith, K. Schulz, and P. S. Jessen, Continuous Nondemolition Measurement of the Cs Clock Transition Pseudospin, Phys. Rev. Lett. **96**, 043001 (2006).

[23] T. Takano, M. Fuyama, R. Namiki, and Y. Takahashi, Spin Squeezing of a Cold Atomic Ensemble with the Nuclear Spin of One-Half, Phys. Rev. Lett. **102**, 033601 (2009).

[24] J. Appel, P. J. Windpassinger, D. Oblak, U. B. Hoff, N. Kjærgaard, and E. S. Polzik, Mesoscopic atomic entanglement for precision measurements beyond the standard quantum limit, Proc. Natl. Acad. Sci. U.S.A. **106**, 10960 (2009).

[25] M. H. Schleier-Smith, I. D. Leroux, and V. Vuletić, States of an Ensemble of Two-Level Atoms with Reduced Quantum Uncertainty, Phys. Rev. Lett. **104**, 073604 (2010).

[26] J. G. Bohnet, K. C. Cox, M. A. Norcia, J. M. Weiner, Z. Chen, and J. K. Thompson, Reduced spin measurement back-action for a phase sensitivity ten times beyond the standard quantum limit, Nat. Photonics **8**, 731 (2014).

[27] O. Hosten, N. J. Engelsen, R. Krishnakumar, and M. A. Kasevich, Measurement noise 100 times lower than the quantum-projection limit using entangled atoms, Nature (London) **529**, 505 (2016).

[28] G. Colangelo, F. M. Ciurana, L. C. Bianchet, R. J. Sewell, and M. W. Mitchell, Simultaneous tracking of spin angle and amplitude beyond classical limits, Nature (London) **543**, 525 (2017).

[29] Q. Y. He, T G. Vaughan, P. D. Drummond, and M. D. Reid, Entanglement, number fluctuations and optimized interferometric phase measurement, New J. Phys. **14**, 093012 (2012).

[30] D. W. Berry and H. M. Wiseman, Optimal States and Almost Optimal Adaptive Measurements for Quantum Interferometry, Phys. Rev. Lett. **85**, 5098 (2000).

[31] M. Kubasik, M. Koschorreck, M. Napolitano, S. R. de Echaniz, H. Crepaz, J. Eschner, E. S. Polzik, and M. W. Mitchell, Polarization-based light-atom quantum interface with an all-optical trap, Phys. Rev. A **79**, 043815 (2009).

[32] J. M. Geremia, J. K. Stockton, and H. Mabuchi, Tensor polarizability and dispersive quantum measurement of multilevel atoms, Phys. Rev. A **73**, 042112 (2006).

[33] I. H. Deutsch and P. S. Jessen, Quantum control and measurement of atomic spins in polarization spectroscopy, Opt. Commun. **283**, 681 (2010).

[34] R. J. Sewell, M. Napolitano, N. Behbood, G. Colangelo, and M. W. Mitchell, Certified quantum non-demolition measurement of a macroscopic material system, Nat. Photonics **7**, 517 (2013).

[35] Y. R. P. Sortais, A. Fuhrmanek, R. Bourgain, and A. Browaeys, Sub-Poissonian atom-number fluctuations using light-assisted collisions, Phys. Rev. A **85**, 035403 (2012).

[36] C.-S. Chuu, F. Schreck, T. P. Meyrath, J. L. Hanssen, G. N. Price, and M. G. Raizen, Direct Observation of Sub-Poissonian Number Statistics in a Degenerate Bose Gas, Phys. Rev. Lett. **95**, 260403 (2005).

[37] F. Gerbier, S. Fölling, A. Widera, O. Mandel, and I. Bloch, Probing Number Squeezing of Ultracold Atoms Across the Superfluid-Mott Insulator Transition, Phys. Rev. Lett. **96**, 090401 (2006).

[38] S. Whitlock, C. F. Ockeloen, and R. J. C. Spreeuw, Sub-Poissonian Atom-Number Fluctuations by Three-Body Loss in Mesoscopic Ensembles, Phys. Rev. Lett. **104**, 120402 (2010).

[39] J.-B. Béguin, E. M. Bookjans, S. L. Christensen, H. L. Sørensen, J. H. Müller, E. S. Polzik, and J. Appel, Generation and Detection of a Sub-Poissonian Atom Number Distribution in a One-Dimensional Optical Lattice, Phys. Rev. Lett. **113**, 263603 (2014).

[40] M. Gajdacz, A. J. Hilliard, M. A. Kristensen, P. L. Pedersen, C. Klempt, J. J. Arlt, and J. F. Sherson, Preparation of Ultracold Atom Clouds at the Shot Noise Level, Phys. Rev. Lett. **117**, 073604 (2016).

[41] M. Koschorreck, M. Napolitano, B. Dubost, and M. W. Mitchell, Quantum Nondemolition Measurement of Large-Spin Ensembles by Dynamical Decoupling, Phys. Rev. Lett. **105**, 093602 (2010).

[42] F. M. Ciurana, G. Colangelo, R. J. Sewell, and M. W. Mitchell, Real-time shot-noise-limited differential photodetection for atomic quantum control, Opt. Lett. **41**, 2946 (2016).

[43] N. Behbood, F. M. Ciurana, G. Colangelo, M. Napolitano, M. W. Mitchell, and R. J. Sewell, Real-time vector field tracking with a cold-atom magnetometer, Appl. Phys. Lett. **102**, 173504 (2013).

[44] N. Behbood, F. M. Ciurana, G. Colangelo, M. Napolitano, Géza Tóth, R. J. Sewell, and M. W. Mitchell, Generation of Macroscopic Singlet States in a Cold Atomic Ensemble, Phys. Rev. Lett. **113**, 093601 (2014).

[45] G. Colangelo, R. J Sewell, N. Behbood, F. M. Ciurana, G. Triginer, and M. W Mitchell, Quantum atom–light interfaces in the gaussian description for spin-1 systems, New J. Phys. **15**, 103007 (2013).

[46] T. W. Kornack, S. J. Smullin, S.-K. Lee, and M. V. Romalis, A low-noise ferrite magnetic shield, Appl. Phys. Lett. **90**, 223501 (2007).

[47] A. Smith, B. E. Anderson, S. Chaudhury, and P. S. Jessen, Three-axis measurement and cancellation of background magnetic fields to less than 50 μg in a cold atom experiment, J. Phys. B **44**, 205002 (2011).

[48] D. J. Wineland, J. J. Bollinger, W. M. Itano, F. L. Moore, and D. J. Heinzen, Spin squeezing and reduced quantum noise in spectroscopy, Phys. Rev. A **46**, R6797 (1992).

[49] D. J. Wineland, J. J. Bollinger, W. M. Itano, and D. J. Heinzen, Squeezed atomic states and projection noise in spectroscopy, Phys. Rev. A **50**, 67 (1994).

[50] I. K. Kominis, T. W. Kornack, J. C. Allred, and M. V. Romalis, A subfemtotesla multichannel atomic magnetometer, Nature (London) **422**, 596 (2003).

[51] J. Lodewyck, P. G. Westergaard, and P. Lemonde, Nondestructive measurement of the transition probability in a Sr optical lattice clock, Phys. Rev. A **79**, 061401 (2009).